Physics of Fluids

Effect of liquid elasticity on nonlinear pressure waves in a viscoelastic bubbly liquid

Cite as: Phys. Fluids **35**, 043309 (2023); https://doi.org/10.1063/5.0131091
Submitted: 18 October 2022 • Accepted: 13 December 2022 • Accepted Manuscript Online: 17 December 2022 • Published Online: 05 April 2023

Takeru Hasegawa (長谷川建) and Tetsuya Kanagawa (金川哲也)

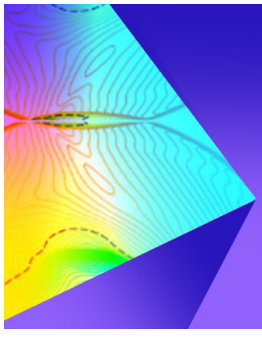

Physics of Fluids ARTICLE scitation.org/journal/phf

Effect of liquid elasticity on nonlinear pressure waves in a viscoelastic bubbly liquid

Cite as: Phys. Fluids **35**, 043309 (2023); doi: 10.1063/5.0131091
Submitted: 18 October 2022 · Accepted: 13 December 2022 ·
Published Online: 5 April 2023

Takeru Hasegawa (長谷川建),[1] and Tetsuya Kanagawa (金川哲也)[2,a)]

AFFILIATIONS

[1]Department of Engineering Mechanics and Energy, Graduate School of Systems and Information Engineering, University of Tsukuba, Tsukuba 305–8573, Japan
[2]Department of Engineering Mechanics and Energy, Institute of Systems and Information Engineering, University of Tsukuba, Tsukuba 305–8573, Japan

[a)]Author to whom correspondence should be addressed: kanagawa.tetsuya.fu@u.tsukuba.ac.jp

ABSTRACT

The importance of viscoelasticity of biological media that are used in medical ultrasounds has been discussed in the literature. Furthermore, the use of microbubbles in biological media drastically improves the efficiency of both diagnostic and therapeutic ultrasounds. Weakly nonlinear wave equations for ultrasound propagation in liquids containing microbubbles have long been studied, although the viscoelasticity of the liquid phase has been ignored for simplicity. In this study, we derived a nonlinear wave equation for ultrasound propagation in a viscoelastic liquid containing microbubbles by considering the effect of the elasticity of the liquid. Additionally, we evaluated how the elasticity of the liquid modifies the nonlinear, dissipation, and dispersion effects of the ultrasound in a few tissue models (i.e., liver, muscle, breast cancer, fat, and skin models and that without shear elasticity). The results revealed that liquid shear elasticity decreases the nonlinear and dissipation effects and increases the dispersion effect, and this tendency is more significantly observed in the breast cancer tissue compared with other tissues. Furthermore, we numerically solved the nonlinear wave equation and investigated the changes in ultrasonic wave evolution with and without shear elasticity.

I. INTRODUCTION

Various types of cavitation phenomena occur in soft tissues. High intensity focused ultrasound (HIFU) is a treatment modality that focuses ultrasound waves on a focal area and ablates the tumor tissue by increasing its temperature.[1–3] However, if there are tissues that absorb or reflect ultrasound waves, such as fat or bone, it is difficult to focus the ultrasound waves, thereby rendering the treatment ineffective as the required temperature would not be reached. However, by injecting microbubbles around the tumor tissue, the thermal effect can be enhanced by the generation of thermal energy owing to the excitation of the microbubble, thus, increasing the therapeutic effect, even when it is difficult to focus the ultrasound wave.[4–9] Histotripsy uses focused ultrasound to generate and collapse cavitation clouds to destroy the tumor tissue in the focal region.[10,11] In recent years, various methods have been developed and experimentally verified to increase the efficiency of tissue fractionation or to shorten the treatment time.[11–14] The difference between HIFU and histotripsy is that HIFU utilizes the thermal effect of cavitation, whereas histotripsy utilizes the mechanical effect of cavitation. The latter is an example of cavitation that causes damage to the body. Extracorporeal shock wave lithotripsy (ESWL) is a treatment modality in which shock waves are irradiated from outside the body to destroy stones, although the normal tissue surrounding the stones can be damaged simultaneously. Moreover, in traumatic brain injury, when a person's head is impacted by a strong force, such as an accident, cavitation can occur inside the skull, which can damage the brain tissue.[15] Furthermore, studies focusing on pressure wave propagation in soft tissues have indicated that shock waves propagating in soft tissues can cause considerable damage.[16–18]

Soft tissues are often considered as viscoelastic bodies containing bubbles. Numerous studies on viscoelastic materials containing bubbles have been conducted in recent years, especially from the viewpoint of multiphase flow. For example, experiments and simulations have been conducted to understand the motion of bubbles in viscoelastic bodies to elucidate the mechanism of cavitation.[15,19–26] Experiments have also been performed to evaluate the material

properties of viscoelastic bodies using cavitation instead of rheometry.[27–34] In those studies, a viscoelastic material model was applied, and the physical properties were estimated by using the data obtained from bubble oscillation.

Pressure waves in liquids containing bubbles have three effects: nonlinear, dissipation, and dispersion. The nonlinear effect in the present context is the effect of steepening the pressure wave, dissipation is the effect of attenuating the pressure wave, and dispersion is the effect of scattering the pressure wave into the waves with various frequency components owing to bubble oscillation. As the characteristics of pressure wave propagation change depending on the balance between the nonlinear, dissipation, and dispersion effects, quantitative evaluation of these three effects is important to accurately predict pressure wave propagation. However, these three effects of pressure waves cannot be measured from experiments. Therefore, a theoretical evaluation method is required. This is made possible using the Korteweg–de Vries–Burgers (KdVB) equation[35] derived by van Wijngaarden, which can be used to evaluate the balance between nonlinear, dissipation, and dispersion effects. The KdVB equation[35] does not include the effect of the elasticity of the liquid, and, to date, there is still no equation that includes it. However, to accurately predict pressure wave propagation in soft tissues while performing HIFU and histotripsy, it is essential to consider the effect of the elasticity of the liquid. Therefore, in this study, we investigate how the nonlinear, dissipation, and dispersion effects change when the effect of liquid shear elasticity is considered and aim to construct a mathematical model that can describe pressure wave propagation in viscoelastic materials containing bubbles.

The paper is organized as follows: In Sec. II, the problem setup and assumptions are clarified, and the basic equations used to formulate the problem are described. In addition, the multiscale method used in the theoretical analysis is described. In Sec. III, the linear wave equation for the near field and the KdVB equation as nonlinear wave equation for the far field are derived, and in Sec. IV, we focused on the coefficients of the derived KdVB equation and discussed how they change in the presence of liquid shear elasticity. In addition, we numerically solved the obtained KdVB equation and considered the change in pressure waves caused by liquid shear elasticity.

II. PROBLEM FORMULATION

A. Problem statement

We considered a weakly nonlinear (i.e., finite but with small amplitude) propagation of plane and progressive pressure wave in a bubbly liquid. In this study, the following assumptions were made for simplicity:

(i) The liquid is slightly compressible.
(ii) The initial flow velocities of gas and liquid phases are zero.
(iii) The number of bubbles is constant, that is, the bubbles do not coalesce, break up, appear, or disappear.
(iv) Only one bubble size is considered, and bubble distribution is spatially uniform.
(v) Bubble–bubble interaction[67] is neglected.
(vi) Mass transport through the bubble–liquid interface[68] is neglected, that is, the number of molecules inside the gas core of each bubble is constant.
(vii) Bubble oscillations are spherically symmetric and are the same in an averaged volume.
(viii) The translation of and drag force on the bubbles[36–38] are neglected.
(ix) The gas inside the bubbles is composed of only non-condensable gas.
(x) The temperature fluctuation of the gas inside the bubble is considered, but the temperature of the liquid phase is assumed to be constant.
(xi) We used the Zener model[39] as the constitutive equation to represent the properties of viscoelastic liquids.
(xii) Shear modulus (i.e., rigidity) of the liquid is considered, but Young's modulus and bulk modulus (i.e., bulk elasticity) of the liquid is neglected for simplicity.

B. Basic equations

The basic equations are composed of nine equations: four conservation equations, bubble dynamics equation, and four constitutive equations. As volumetric-averaged equations based on a two-fluid model[40,41] to describe the dependence of the initial void fraction[42] were used, conservation laws of mass and momentum for gas and liquid phases are first introduced as follows:

$$\frac{\partial}{\partial t^*}\left(\alpha\rho_{\mathrm{G}}^*\right)+\frac{\partial}{\partial x^*}\left(\alpha\rho_{\mathrm{G}}^* u_{\mathrm{G}}^*\right)=0, \tag{1}$$

$$\frac{\partial}{\partial t^*}\left[(1-\alpha)\rho_{\mathrm{L}}^*\right]+\frac{\partial}{\partial x^*}\left[(1-\alpha)\rho_{\mathrm{L}}^* u_{\mathrm{L}}^*\right]=0, \tag{2}$$

$$\frac{\partial}{\partial t^*}\left(\alpha\rho_{\mathrm{G}}^* u_{\mathrm{G}}^*\right)+\frac{\partial}{\partial x^*}\left(\alpha\rho_{\mathrm{G}}^* u_{\mathrm{G}}^{*2}\right)+\alpha\frac{\partial p_{\mathrm{G}}^*}{\partial x^*}=F^*, \tag{3}$$

$$\frac{\partial}{\partial t^*}\left[(1-\alpha)\rho_{\mathrm{L}}^* u_{\mathrm{L}}^*\right]+\frac{\partial}{\partial x^*}\left[(1-\alpha)\rho_{\mathrm{L}}^* u_{\mathrm{L}}^{*2}\right]+(1-\alpha)\frac{\partial p_{\mathrm{L}}^*}{\partial x^*}+P^*\frac{\partial\alpha}{\partial x^*}=-F^*, \tag{4}$$

where t^* is the time, x^* is the space coordinate, α is the void fraction, ρ^* is the density, u^* is the fluid velocity, p^* is the pressure, and P^* is the surface-averaged pressure.[43] The subscript $*$ denotes a dimensional quantity, and the subscripts G and L denote the gas and liquid phases, respectively. As the interfacial transport term of momentum F^*, we used the virtual mass force model as follows:[41,43–45]

$$F^*=-\beta_1\alpha\rho_{\mathrm{L}}^*\left(\frac{\mathrm{D_G}u_{\mathrm{G}}^*}{\mathrm{D}t^*}-\frac{\mathrm{D_L}u_{\mathrm{L}}^*}{\mathrm{D}t^*}\right)-\beta_2\rho_{\mathrm{L}}^*\left(u_{\mathrm{G}}^*-u_{\mathrm{L}}^*\right)\frac{\mathrm{D_G}\alpha}{\mathrm{D}t^*}-\beta_3\alpha\left(u_{\mathrm{G}}^*-u_{\mathrm{L}}^*\right)\frac{\mathrm{D_G}\rho_{\mathrm{L}}^*}{\mathrm{D}t^*}, \tag{5}$$

where β_1, β_2, and β_3 are the virtual mass coefficients and are 1/2 in the case of spherical bubbles. Furthermore, $\mathrm{D_G}/\mathrm{D}t^*$ or $\mathrm{D_L}/\mathrm{D}t^*$ are material derivatives of the gas and liquid phases, respectively, and are given as follows:

$$\frac{\mathrm{D_G}}{\mathrm{D}t^*}\equiv\frac{\partial}{\partial t^*}+u_{\mathrm{G}}^*\frac{\partial}{\partial x^*},\quad \frac{\mathrm{D_L}}{\mathrm{D}t^*}\equiv\frac{\partial}{\partial t^*}+u_{\mathrm{L}}^*\frac{\partial}{\partial x^*}. \tag{6}$$

For bubble dynamics, we utilized the modified Keller equation (7), which was derived by adding the terms that are attributed to liquid shear elasticity[46] to the original Keller equation[47,48] for spherically symmetric volume oscillations of bubbles in a compressible liquid,[46]

$$\left(1-\frac{1}{c_{L0}^*}\frac{D_G R^*}{Dt^*}\right)R^*\frac{D_G{}^2R^*}{Dt^{*2}}+\frac{3}{2}\left(1-\frac{1}{3c_{L0}^*}\frac{D_G R^*}{Dt^*}\right)\left(\frac{D_G R^*}{Dt^*}\right)^2 = \frac{1}{\rho_{L0}^*}\left(1+\frac{1}{c_{L0}^*}\frac{D_G R^*}{Dt^*}\right)\left(P^*-\tau_{rr}^*|_{R^*}+3q^*\right) + \frac{R^*}{\rho_{L0}^* c_{L0}^*}\frac{D_G}{Dt^*}\left(p_L^*+P^*-\tau_{rr}^*|_{R^*}+3q^*\right), \quad (7)$$

where c_{L0}^* is the speed of sound in the pure liquid, R^* is the bubble radius, $\tau_{rr}^*|_{R^*}$ is the radial component of the deviatoric stress at the bubble wall, the subscript 0 denotes the initial quantity, and q^* is defined as

$$q^*(R^*,t^*)\equiv\int_{R^*}^{\infty}\frac{\tau_{rr}^*}{r^*}dr^*, \quad (8)$$

where r^* is the radial distance from the center of the bubble.

As in our recent reports,[49–51] the energy equation[52] for thermal conduction at the bubble–liquid interface was used to express the thermal effect inside the bubble as

$$\frac{D_G p_G^*}{Dt^*}=\frac{3}{R^*}\left[(\kappa-1)\lambda_G^*\left.\frac{\partial T_G^*}{\partial r^*}\right|_{r^*=R^*}-\kappa p_G^*\frac{D_G R^*}{Dt^*}\right], \quad (9)$$

where T_G^* is the temperature of the gas phase, κ is the ratio of specific heats, and λ_G^* is the thermal conductivity of the gas phase. The temperature gradient term $\partial T_G^*/\partial r^*|_{r^*=R^*}$ was rewritten by using the following model given by Sugiyama *et al.*,[53]

$$\left.\frac{\partial T_G^*}{\partial r^*}\right|_{r^*=R^*}=\frac{\mathrm{Re}(\tilde{L}_p^*)(T_0^*-T_G^*)}{|\tilde{L}_p^*|^2}+\frac{\mathrm{Im}(\tilde{L}_p^*)}{\omega_B^*|\tilde{L}_p^*|^2}\frac{D_G T_G^*}{Dt^*}, \quad (10)$$

where T_0^* is the initial temperature of the liquid and gas phases, $\tilde{L}_p^*$ is the complex number with the length dimension defined in Ref. 53, and $\mathrm{Re}(\tilde{L}_p^*)$ and $\mathrm{Im}(\tilde{L}_p^*)$ are the real and imaginary parts of $\tilde{L}_p^*$, respectively, and ω^* is the typical angular frequency.

In this paper, the linear natural angular frequency of a single bubble oscillation, ω_B^*, is introduced by

$$\omega_B^*\equiv\sqrt{\frac{3\gamma_e p_{G0}^*-2\sigma^*/R_0^*+4G^*}{\rho_{L0}^* R_0^{*2}}-\left(\frac{2\mu_{e0}^*}{\rho_{L0}^* R_0^{*2}}\right)^2}, \quad (11)$$

where γ_e is the effective polytropic exponent and μ_{e0}^* is the initial effective viscosity.[53] Equation (11) was defined by adding the term of liquid shear modulus G^* to the linear natural angular frequency of a single bubble oscillation, as defined in Ref. 53. Table I shows the linear natural angular frequency ω_B^* for different types of biological soft tissues. In this study, for simplicity, we regard biological soft tissues as a viscoelastic liquid. In Table I, the initial density and the initial speed of sound in the liquid vary among different types of biological tissues, with Wells and Liang[54] reporting densities in the range of 916–1060 kg/m^3 and speed of sounds in the range of 1412–1629 m/s. However, since specific values for the density and the speed of sound of each tissue were not given, the density and the speed of sound were calculated here as 1000 kg/m^3 and 1500 m/s, respectively, for all biological tissues. The values for viscosity and relaxation time were taken from Zilonova *et al.*[39,55] and were assumed to be the same for all biological soft tissues. Temperature was assumed to be human body temperature.

TABLE I. The linear natural angular frequency ω_B^* for the case of $\alpha_0=1.0\times10^{-5}$, $R_0^*=100\,\mu$m, $\rho_{L0}^*=1000.0$ kg/m^3, $c_{L0}^*=1500.0$ m/s, $p_{L0}^*=101\,325$ Pa, $\sigma^*=0.056$ N/m, $\mu^*=0.015$ Pa·s, $\lambda^*=1.0\times10^{-7}$ s, $T_0^*=310.15$ K, $\lambda_G^*=0.0241$ W/(m K), and $\kappa=1.4$; noting that these values except for G^* are used to calculate ω_B^* of every tissue. As these tissues can be regarded as incompressible,[54] we used the relationship between Young's modulus E^* and shear modulus G^*, $G^*\approx E^*/3$.[54] As the shear modulus of the liquid-phase biological soft tissue increased, ω_B^* also increased. Of note, Figs. 1–3 demonstrate the same calculation conditions as those in Table I, unless otherwise indicated.

Tissue	Shear modulus G^* [kPa]	ω_B^* [MHz]
Without shear elasticity	0	0.197
Skin[62]	0.37	0.198
Fat[63]	3.3	0.201
Liver[54]	4.3	0.202
Muscle[54]	6.7	0.205
Breast cancer[54]	31	0.228

We compared six cases: five types of soft tissues detailed in Table I and a tissue model "without shear elasticity" that corresponds to $G^*=0$. Here, without shear elasticity is a case in which the density, sound velocity, and viscosity are the same as those of other biological soft tissues, but G^* is set to zero. Although this is a hypothetical case that differs from the actual biological soft tissues, it was chosen for the purpose of focusing attention on the effects of shear elasticity. We found that ω_B^* increased as the shear modulus of the medium increased.

The following constitutive equations close (1)–(9):

(i) The Tait equation for the liquid state is

$$p_L^*=p_{L0}^*+\frac{\rho_{L0}^* c_{L0}^{*2}}{n}\left[\left(\frac{\rho_L^*}{\rho_{L0}^*}\right)^n-1\right], \quad (12)$$

where n is material constant, for example, $n=7.15$ for water.

(ii) The equation for the gaseous state is

$$\frac{p_G^*}{p_{G0}^*}=\frac{\rho_G^*}{\rho_{G0}^*}\frac{T_G^*}{T_0^*}. \quad (13)$$

(iii) The conservation law of mass inside the bubble is

$$\frac{\rho_G^*}{\rho_{G0}^*}=\left(\frac{R_0^*}{R^*}\right)^3. \quad (14)$$

(iv) The balance of normal stress across the bubble–liquid interface is

$$p_G^*-\left(p_L^*+P^*\right)=\frac{2\sigma^*}{R^*}-\tau_{rr}^*|_{R^*}, \quad (15)$$

where σ^* is the surface tension.

C. Constitutive equation

We utilized two equations[39] derived from the constitutive equation of the Zener model. Although there are various models to describe viscoelastic materials, such as the linear Maxwell model[56] and the neo-Hookean model,[22] we utilized the Zener model in this study because it is widely used in experiments and simulations using gels and

phantoms that imitate soft tissues.[57–60] In this study, the Zener model was used as the constitutive equation for viscoelasticity because soft tissues are assumed to be the primary area of application of ultrasound waves in this study,

$$q^* + \lambda^* \frac{\mathrm{D_G} q^*}{\mathrm{D}t^*} + \lambda^* \frac{1}{R^*} \frac{\mathrm{D_G} R^*}{\mathrm{D}t^*} \tau^*_{rr}|_{R^*} = \frac{1}{3}\left[-\frac{4G^*}{3R^{*3}} \left(R^{*3} - R_0^{*3} \right) - 4\mu^* \frac{1}{R^*} \frac{\mathrm{D_G} R^*}{\mathrm{D}t^*} \right], \tag{16}$$

$$\left(1 + 3\lambda^* \frac{1}{R^*} \frac{\mathrm{D_G} R^*}{\mathrm{D}t^*} \right) \tau^*_{rr}|_{R^*} + \lambda^* \frac{\mathrm{D_G} \tau^*_{rr}|_{R^*}}{\mathrm{D}t^*} = -\frac{4G^*}{3} \left[1 - \left(\frac{R_0^*}{R^*} \right)^3 \right] - 4\mu^* \frac{1}{R^*} \frac{\mathrm{D_G} R^*}{\mathrm{D}t^*}, \tag{17}$$

where μ^* is the liquid viscosity, G^* is the liquid shear modulus, and λ^* is the relaxation time of the liquid.

Although we represent the material derivative of q^* and $\tau^*_{rr}|_{R^*}$ as $\mathrm{D_G} q^*/\mathrm{D}t^*$ and $\mathrm{D_G} \tau^*_{rr}|_{R^*}/\mathrm{D}t^*$, the material derivative of q^* and $\tau^*_{rr}|_{R^*}$ as $\mathrm{D_G}/\mathrm{D}t^*$ or $\mathrm{D_L}/\mathrm{D}t^*$ has not been strictly determined. This causes a difference in the advection term of the material derivative. However, owing to the order evaluation in this study, the contribution of the advection term can be neglected and material derivatives of q^* and $\tau^*_{rr}|_{R^*}$ do not affect the results.

D. Multiple scale analysis

To focus on the low-frequency long wave, the scaling relations of nondimensional ratios among the physical parameters are defined as follows:[61]

$$\left(\frac{R_0^*}{L^*}, \frac{\omega^*}{\omega_\mathrm{B}^*}, \frac{U^*}{c_{\mathrm{L}0}^*} \right) \equiv \left(O(\sqrt{\epsilon}), O(\sqrt{\epsilon}), O(\sqrt{\epsilon}) \right) \equiv \left(\Delta\sqrt{\epsilon}, \Omega\sqrt{\epsilon}, V\sqrt{\epsilon} \right), \tag{18}$$

where ϵ is a nondimensional wave amplitude ($0 < \epsilon \ll 1$), Δ, Ω, and V are the constants of $O(1)$, R_0^* is the radius of a typical bubble, L^* is the typical wavelength, and U^* is the typical wave propagation speed.

Independent variables t^* and v^* are nondimensionalized as follows:

$$t \equiv \frac{t^*}{T^*}, \quad x \equiv \frac{x^*}{L^*}, \tag{19}$$

where T^* is the typical period of a propagating wave, which is related to the wavelength L^* and the wave propagation speed U^* through $T^* \equiv L^*/U^*$. The near field [i.e., the temporal and spatial scales of $O(1)$] is defined as

$$t_0 = t, \quad x_0 = x, \tag{20}$$

and the far field [i.e., the temporal and spatial scales of $O(1/\epsilon)$] is described as

$$t_1 = \epsilon t, \quad x_1 = \epsilon x. \tag{21}$$

Using (20) and (21) with the derivative expansion method,[64] the differential operators are expanded as follows:

$$\frac{\partial}{\partial t} = \frac{\partial}{\partial t_0} + \epsilon \frac{\partial}{\partial t_1}, \quad \frac{\partial}{\partial x} = \frac{\partial}{\partial x_0} + \epsilon \frac{\partial}{\partial x_1}. \tag{22}$$

Furthermore, the dependent variables are nondimensionalized and expanded in the power series of ϵ as follows:

$$\frac{\alpha}{\alpha_0} = 1 + \epsilon\alpha_1 + \epsilon^2\alpha_2 + \cdots, \tag{23}$$

$$\frac{R^*}{R_0^*} = 1 + \epsilon R_1 + \epsilon^2 R_2 + \cdots, \tag{24}$$

$$\frac{u_\mathrm{G}^*}{U^*} = \epsilon u_{\mathrm{G}1} + \epsilon^2 u_{\mathrm{G}2} + \cdots, \tag{25}$$

$$\frac{u_\mathrm{L}^*}{U^*} = \epsilon u_{\mathrm{L}1} + \epsilon^2 u_{\mathrm{L}2} + \cdots, \tag{26}$$

$$\frac{p_\mathrm{L}^*}{\rho_{\mathrm{L}0}^* U^{*2}} = p_{\mathrm{L}0} + \epsilon p_{\mathrm{L}1} + \epsilon^2 p_{\mathrm{L}2} + \cdots, \tag{27}$$

$$\frac{\rho_\mathrm{L}^*}{\rho_{\mathrm{L}0}^*} = 1 + \epsilon^2 \rho_{\mathrm{L}1} + \epsilon^3 \rho_{\mathrm{L}2} + \cdots, \tag{28}$$

$$\frac{\tau^*_{rr}|_{R^*}}{\rho_{\mathrm{L}0}^* U^{*2}} = \tau_0 + \epsilon\tau_1 + \epsilon^2\tau_2 + \cdots, \tag{29}$$

$$\frac{q^*}{\rho_{\mathrm{L}0}^* U^{*2}} = q_0 + \epsilon q_1 + \epsilon^2 q_2 + \cdots, \tag{30}$$

$$\frac{T_\mathrm{G}^*}{T_0^*} = 1 + \epsilon T_{\mathrm{G}1} + \epsilon^2 T_{\mathrm{G}2} + \cdots. \tag{31}$$

The liquid viscosity μ^*, the surface tension σ^*, the liquid shear modulus G^*, and the relaxation time of the liquid λ^* are nondimensionalized as

$$\frac{\mu^*}{\rho_{\mathrm{L}0}^* U^* L^*} \equiv O(\epsilon) \equiv \mu\epsilon, \tag{32}$$

$$\frac{\sigma^*}{\rho_{\mathrm{L}0}^* U^{*2} R_0^*} \equiv O(1) \equiv \sigma, \tag{33}$$

$$\frac{G^*}{\rho_{\mathrm{L}0}^* U^{*2}} \equiv O(1) \equiv G, \tag{34}$$

$$\frac{\lambda^*}{T^*} \equiv O(\epsilon) \equiv \lambda\epsilon. \tag{35}$$

The nondimensional pressures for the gas and liquid phases in the unperturbed states $p_{\mathrm{G}0}^*$ and $p_{\mathrm{L}0}^*$ are defined as

$$\frac{p_{\mathrm{G}0}^*}{\rho_{\mathrm{L}0}^* U^{*2}} \equiv O(1) \equiv p_{\mathrm{G}0}, \quad \frac{p_{\mathrm{L}0}^*}{\rho_{\mathrm{L}0}^* U^{*2}} \equiv O(1) \equiv p_{\mathrm{L}0}. \tag{36}$$

III. DERIVATION OF KdVB EQUATION

A. Leading order of approximation

Substituting (5), (6), and (10)–(36) into (1)–(4), (7)–(9), (16), and (17) and collecting the $O(\epsilon^1)$ terms, the following system of linearized equations for the first-order problem were obtained:

(i) Mass conservation law in the gas phase,

$$\frac{\partial \alpha_1}{\partial t_0} - 3\frac{\partial R_1}{\partial t_0} + \frac{\partial u_{\mathrm{G}1}}{\partial x_0} = 0. \tag{37}$$

(ii) Mass conservation law in the liquid phase,

$$\alpha_0 \frac{\partial \alpha_1}{\partial t_0} - (1 - \alpha_0) \frac{\partial u_{\mathrm{L}1}}{\partial x_0} = 0. \tag{38}$$

(iii) Momentum conservation law in the gas phase,

$$\beta_1 \frac{\partial u_{\mathrm{G}1}}{\partial t_0} - \beta_1 \frac{\partial u_{\mathrm{L}1}}{\partial t_0} - 3p_{\mathrm{G}0} \frac{\partial R_1}{\partial x_0} + p_{\mathrm{G}0} \frac{\partial T_{\mathrm{G}1}}{\partial x_0} = 0. \tag{39}$$

(iv) Momentum conservation law in the liquid phase,

$$(1-\alpha_0+\beta_1\alpha_0)\frac{\partial u_{L1}}{\partial t_0}-\beta_1\alpha_0\frac{\partial u_{G1}}{\partial t_0}+(1-\alpha_0)\frac{\partial p_{L1}}{\partial x_0}=0. \quad (40)$$

(v) Modified Keller equation,

$$p_{G0}T_{G1}+\left[3(\gamma_e-1)p_{G0}-\frac{\Delta^2}{\Omega^2}\right]R_1-p_{L1}+\frac{4\mu_{e0}^2}{\Delta^2}=0. \quad (41)$$

(vi) Energy equation for thermal conduction at the bubble–liquid interface,

$$\frac{\partial T_{G1}}{\partial t_0}+3(\kappa-1)\frac{\partial R_1}{\partial t_0}=0. \quad (42)$$

The system of linearized equations, i.e., (37)–(42) contained six dependent variables (i.e., α_1, p_{L1}, u_{G1}, u_{L1}, T_{G1}, and R_1). By eliminating α_1, p_{L1}, u_{G1}, u_{L1}, and T_{G1}, the linear wave equation for the first-order perturbation of the bubble radius R_1 was derived as follows:

$$\frac{\partial^2 R_1}{\partial t_0^2}-v_p^2\frac{\partial^2 R_1}{\partial x_0^2}=0, \quad (43)$$

where the phase velocity v_p is given by,

$$v_p\equiv\sqrt{\frac{3\alpha_0(1-\alpha_0+\beta_1)\kappa p_{G0}-\beta_1(1-\alpha_0)\left[3(\gamma_e-\kappa)p_{G0}-\Delta^2/\Omega^2\right]}{3\beta_1\alpha_0(1-\alpha_0)}}. \quad (44)$$

By substituting the definitions of p_{G0} in (36), Δ and Ω in (18) into (44), we formulated a typical propagation speed U^* as follows:

$$U^*=\sqrt{\frac{3\alpha_0(1-\alpha_0+\beta_1)\kappa p_{G0}^*/\rho_{L0}^*-\beta_1(1-\alpha_0)\left[3(\gamma_e-\kappa)p_{G0}^*/\rho_{L0}^*-R_0^{*2}\omega_B^{*2}\right]}{3\beta_1\alpha_0(1-\alpha_0)}}. \quad (45)$$

Figure 1 shows the propagation speed U^* vs the initial void fraction α_0. We found that U^* increases as the liquid shear elasticity increases.

Next, we introduced the following variable transformation:

$$\varphi_0\equiv x_0-t_0. \quad (46)$$

By setting $R_1\equiv f(\varphi_0;x_1,t_1)$, the remainder of the dependent variables can be rewritten in terms of $R_1=f$ as follows:

$$\alpha_1=s_1 f,\quad u_{G1}=s_2 f,\quad u_{L1}=s_3 f,\quad p_{L1}=s_4 f,\quad T_{G1}=s_5 f, \quad (47)$$

with

$$s_5=-3(\kappa-1),\quad s_4=3(\gamma_e-\kappa)p_{G0}-\frac{\Delta^2}{\Omega^2},$$
$$s_1=\frac{(1-\alpha_0)[3\beta_1\alpha_0-(1-\alpha_0)s_4]}{\alpha_0(1-\alpha_0+\beta_1)},\quad (48)$$
$$s_2=s_1-3,\quad s_3=-\frac{\alpha_0 s_1}{1-\alpha_0}.$$

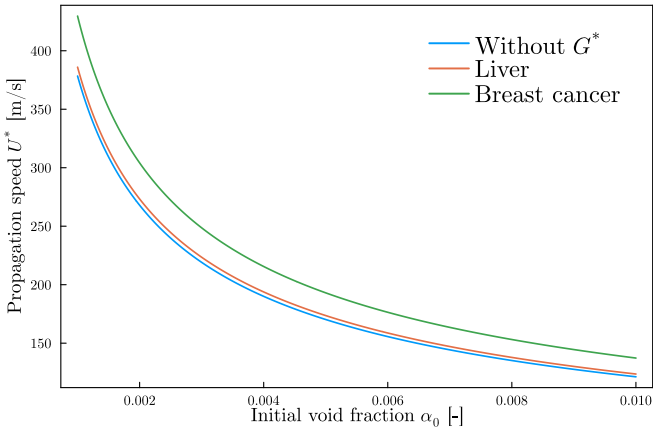

FIG. 1. Propagation speed U^* vs initial void fraction in the liver, breast cancer, and the tissue model without shear elasticity. Note that "Without G^*" means "Without shear elasticity" in Figs. 1 and 2. Clearly, U^* increased as the liquid shear elasticity increased.

B. Second order of approximation

Following the procedure presented in Sec. III A but for the $O(\epsilon^2)$ terms, the following system of equations as a counterpart of $O(\epsilon)$ for the second-order problem were obtained:

$$\frac{\partial \alpha_2}{\partial t_0}-3\frac{\partial R_2}{\partial t_0}+\frac{\partial u_{G2}}{\partial x_0}=K_1, \quad (49)$$

$$\alpha_0\frac{\partial \alpha_2}{\partial t_0}-(1-\alpha_0)\frac{\partial u_{L2}}{\partial x_0}=K_2, \quad (50)$$

$$\beta_1\frac{\partial u_{G2}}{\partial t_0}-\beta_1\frac{\partial u_{L2}}{\partial t_0}-3p_{G0}\frac{\partial R_2}{\partial x_0}+p_{G0}\frac{\partial T_{G2}}{\partial x_0}=K_3, \quad (51)$$

$$(1-\alpha_0+\beta_1\alpha_0)\frac{\partial u_{L2}}{\partial t_0}-\beta_1\alpha_0\frac{\partial u_{G2}}{\partial t_0}+(1-\alpha_0)\frac{\partial p_{L2}}{\partial x_0}=K_4, \quad (52)$$

$$p_{G0}T_{G2}+\left[3(\gamma_e-1)p_{G0}-\frac{\Delta^2}{\Omega^2}\right]R_2-p_{L2}=K_5, \quad (53)$$

$$\frac{\partial T_{G2}}{\partial t_0}+3(\kappa-1)\frac{\partial R_2}{\partial t_0}=K_6, \quad (54)$$

where the explicit forms of the inhomogeneous terms K_i (i=1, 2, 3, 4, 5, 6) are presented in Appendix A. Equations (49)–(54) are combined into a single equation as follows:

$$\frac{\partial^2 R_2}{\partial t_0^2} - v_p^2 \frac{\partial^2 R_2}{\partial x_0^2} = K(f; \varphi_0, x_1, t_1)$$
$$= -\frac{1}{3}\frac{\partial K_1}{\partial t_0} + \frac{1}{3\alpha_0}\frac{\partial K_2}{\partial t_0} + \frac{1-\alpha_0+\beta_1}{3\beta_1(1-\alpha_0)}\frac{\partial K_3}{\partial x_0}$$
$$+ \frac{1}{3\alpha_0(1-\alpha_0)}\frac{\partial K_4}{\partial x_0} + \frac{1}{3\alpha_0}\frac{\partial^2 K_5}{\partial x_0^2}$$
$$- \frac{\alpha_0(1-\alpha_0)+\beta_1}{3\beta_1\alpha_0(1-\alpha_0)} p_{G0} \int \frac{\partial^2 K_6}{\partial x_0^2} \mathrm{d}t_0. \quad (55)$$

From the solvability condition of the inhomogeneous equation in (55), which is also the nonsecular condition for the asymptotic expansions in (23)–(31), we have $K = 0$. By using (46)–(48) and setting $v_p \equiv 1$, the following equation is obtained:

$$2\frac{\partial}{\partial \varphi_0}\left(\frac{\partial f}{\partial t_1} + \frac{\partial f}{\partial v_1} + \Pi_0 \frac{\partial f}{\partial \varphi_0} + \Pi_1 f \frac{\partial f}{\partial \varphi_0} + \Pi_{21}\frac{\partial^2 f}{\partial \varphi_0^2} + \Pi_{22} f + \Pi_3 \frac{\partial^3 f}{\partial \varphi_0^3}\right) = 0. \quad (56)$$

Finally, through a variable transformation,

$$\tau = \epsilon t, \quad \xi = x - (1 + \epsilon\Pi_0)t, \quad (57)$$

the KdVB equation for nonlinear propagation in the far field can be obtained as follows:

$$\frac{\partial f}{\partial \tau} + \Pi_1 f \frac{\partial f}{\partial \xi} + \Pi_{21}\frac{\partial^2 f}{\partial \xi^2} + \Pi_{22} f + \Pi_3 \frac{\partial^3 f}{\partial \xi^3} = 0, \quad (58)$$

where Π_1 is the nonlinear coefficient, Π_{21} is the dissipation coefficient due to viscosity and acoustic radiation of the oscillating bubbles in a compressible liquid, Π_{22} is the dissipation coefficient due to thermal conduction at the bubble–liquid interface, and Π_3 is the dispersion coefficient. The explicit forms of $\Pi_i\,(i = 0, 1, 21, 22, 3)$ are expressed as

$$\Pi_0 = \frac{1-\alpha_0}{6\alpha_0} V^2 \left[3(\gamma_e - \kappa)p_{G0} - \frac{\Delta^2}{\Omega^2}\right] + \frac{2\mu_{e0}^2}{3\alpha_0\Delta^2}$$
$$+ \frac{\alpha_0(1-\alpha_0)+\beta_1}{2\beta_1\alpha_0(1-\alpha_0)}(\kappa - 1)\zeta_{STM2}\, p_{G0}, \quad (59)$$

$$\Pi_1 = \frac{1}{6}\left\{k_1 - \frac{k_2}{\alpha_0} + \frac{(1-\alpha_0+\beta_1)k_3}{\beta_1(1-\alpha_0)} + \frac{k_4}{\alpha_0(1-\alpha_0)} - \frac{2\Delta^2}{\alpha_0\Omega^2}k_5 + \frac{[\alpha_0(1-\alpha_0)+\beta_1]p_{G0}}{\beta_1\alpha_0(1-\alpha_0)}k_6\right\}, \quad (60)$$

$$\Pi_{21} = -\frac{1}{6\alpha_0}\left[4\mu + \frac{\Delta^3 V}{\Omega^2} + 3(\kappa - \gamma_e)\Delta V p_{G0} - 4\lambda G\right], \quad (61)$$

$$\Pi_{22} = \frac{\alpha_0(1-\alpha_0)+\beta_1}{2\beta_1\alpha_0(1-\alpha_0)}(\kappa - 1)\zeta_{STM1}\, p_{G0}, \quad (62)$$

$$\Pi_3 = \frac{\Delta^2}{6\alpha_0}, \quad (63)$$

where the explicit forms of $k_i\ (i = 1, 2, 3, 4, 5, 6)$ are written as

$$k_1 = 6(2 - s_1) + 2s_2(3 - s_1), \quad (64)$$

$$k_2 = -2\alpha_0 s_1 s_3, \quad (65)$$

$$\hat{k} = (\beta_1 + \beta_2)(s_2 - s_3)s_1 - \beta_1(s_2^2 - s_3^2), \quad (66)$$

$$k_3 + \hat{k} + [3(s_1 - 4) + (6 - s_1)s_5]p_{G0}, \quad (67)$$

$$k_4 = -\alpha_0\hat{k} + \alpha_0 s_1 s_4 - 2(1-\alpha_0)s_3^2 - 2\alpha_0 s_1 s_3, \quad (68)$$

$$k_5 = 1 + \frac{3\Omega^2}{\Delta^2}(3\kappa + 1 - \gamma_e)p_{G0} + 4\frac{\Omega^2}{\Delta^2}G, \quad (69)$$

$$k_6 = 3(\kappa - 1)(3\kappa - 4 + 2s_5). \quad (70)$$

These coefficients mainly depend on the initial void fraction and the initial bubble radius.

IV. DISCUSSION

A. Effects of liquid shear elasticity

In this section, we focus on the change in the value of $\Pi_i\,(i = 1, 21, 22, 3)$ and discuss the effect of liquid shear elasticity on the nonlinear, dissipation, and dispersion effects of the pressure waves. First, to visualize the change in the coefficients Π_i in terms of liquid shear elasticity, we compared the coefficient–initial void fraction α_0 curves for six different liquid phases: tissue without shear elasticity, skin, fat, liver, muscle, and breast cancer tissues. All these models have the same material properties (shown in the caption of Table I) except for the shear modulus G^*. The shear modulus G^* of the liver, muscle, breast cancer tissue, fat, and skin are shown in Table I.[54,62,63] As these soft tissues are the target areas of pressure waves or tissues through which the pressure waves pass while applying therapeutic methods, such as HIFU and histotripsy, it is important to investigate their characteristics of pressure wave propagation.

Figure 2 shows the relationship between the magnitude of coefficient $\Pi_i\,(i = 1, 21, 22, 3)$ and the initial void fraction α_0. The void fraction was considered in the range of 10^{-6} to 10^{-2}. We observed that the coefficient values of all coefficients changed in the range of a large void fraction; however, in the range of a small void fraction, the coefficient values were almost constant. We then focused on the effect of liquid shear elasticity. As shown in Fig. 2, in all cases with shear elasticity shown in Table I, the magnitudes of the nonlinear coefficients, dissipation coefficients due to viscosity and acoustic radiation, and dissipation coefficients due to thermal conduction at the bubble–liquid interface are smaller, and the dispersion coefficient is larger than in the case without shear elasticity. This indicates that the shear elasticity of the liquid phase decreases the nonlinear and dissipation effects and increases the dispersion effect. Moreover, Table I shows that the shear modulus of breast cancer is larger than that of skin, and Fig. 2 shows that the difference in coefficients between the breast cancer case and the without shear elasticity case is greater than the difference in coefficients between the skin case and the without shear elasticity case, and these tendencies are also observed in the other biological soft tissues. This suggests that the coefficients change more significantly as shear modulus of tissue is larger.

To quantitatively consider the effect of liquid shear elasticity on the nonlinear, dissipation, and dispersion effects of the pressure wave, we investigated the change in the coefficients Π_i depending on whether the shear elasticity is considered. We compared the tissue model without shear elasticity with the breast cancer tissue because, among the five types of soft tissues described in Table I, the rate of change in coefficients was the largest in the breast cancer tissue. Table II shows the result of comparison of the coefficients between the breast cancer tissue and the tissue without shear elasticity.

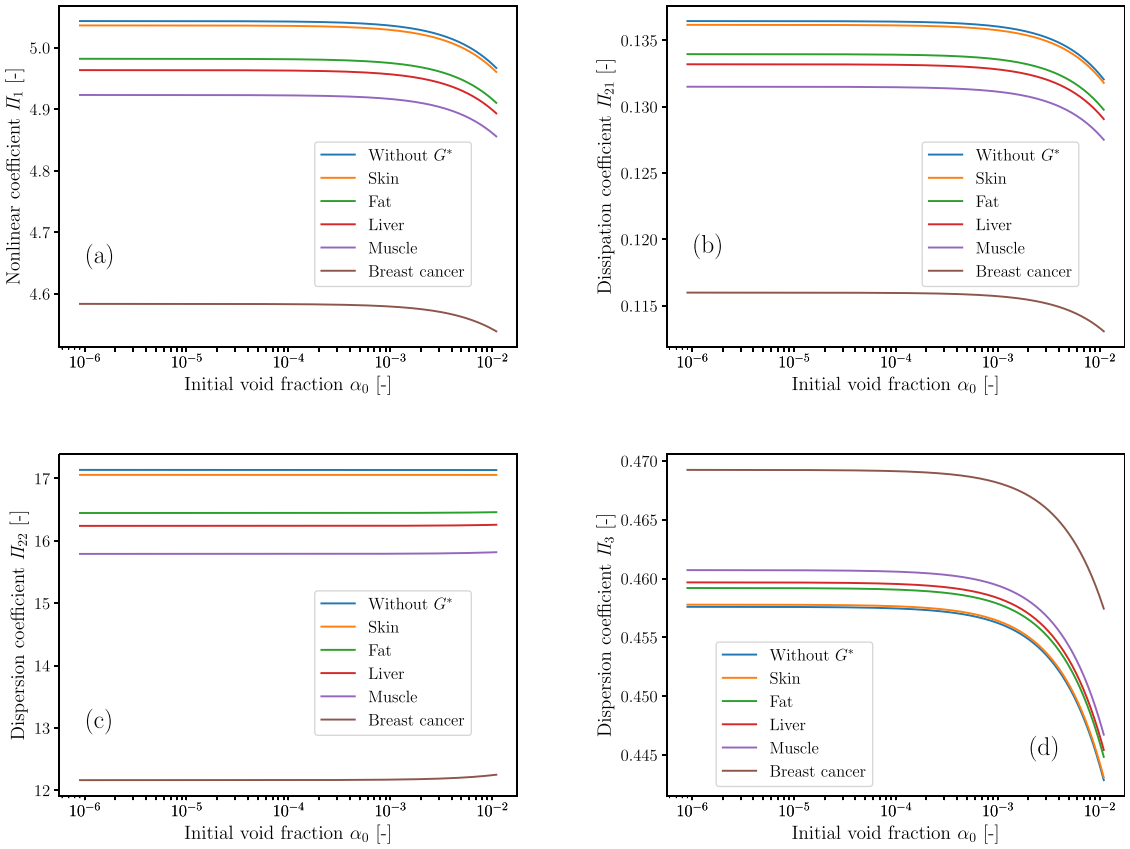

FIG. 2. (a) Nonlinear, (b) and (c) dissipation, and (d) dispersion coefficients vs the initial void fraction α_0 of the liver, muscle, breast cancer tissue, fat, skin, and the tissue without shear elasticity. The liquid shear elasticity decreases the nonlinear and dissipation effects and increases the dispersion effect, and this tendency becomes prominent for the case in which the liquid shear elasticity increases.

Figure 2 and Table II suggest that liquid shear elasticity has an effect on all the coefficients, that is, liquid shear elasticity decreases the nonlinear and dissipation effects of pressure waves, whereas it increases the dispersion effect.

B. Numerical solution

In this section, we numerically solved the obtained KdVB equation (58) and showed the result of temporal evolution of the pressure waves by comparing the waveform of the liquid between the breast cancer tissue and the tissue without shear elasticity. We utilized the split-step Fourier method[65,66] to solve the equation. The detailed numerical scheme is described in the Appendix B.

Figure 3 is the numerical solution of (58) at $\tau = 0.0$, 0.5, 1.5, and 4.0. The red and black waveforms represent the waveforms with and without liquid shear elasticity, respectively. We set the initial waveform as a shock wave [Fig. 3(a)]. In Fig. 3(b), each of the two waveforms splits into pulses, suggesting that the dispersion effect is in effect. However, no a significant difference is observed between them. In Fig. 3(c) and 3(d), some difference in attenuation is observed. In particular, near $\xi = 0$ in Fig. 3(d), a pulse-like waveform was observed in the tissue with liquid shear elasticity, whereas a flattened waveform was observed in the tissue without shear elasticity. This suggests that attenuation of the wave is suppressed owing to the liquid shear elasticity; this is consistent with the decrease in the magnitude of the dissipation coefficients discussed in Sec. IV A.

TABLE II. The ratio of variation of the coefficient owing to the consideration of shear elasticity. Each ratio is defined as $\Pi_{i,\mathrm{w}}/\Pi_{i,\mathrm{wo}}$ $(i = 1, 21, 22, 3)$, $\Pi_{i,\mathrm{w}}$ is the coefficient of the tissue with shear elasticity (i.e., the breast cancer tissue), and $\Pi_{i,\mathrm{wo}}$ is the coefficient of the tissue without shear elasticity.

Coefficient	Ratio [%]
Π_1	−9.12
Π_{21}	−14.99
Π_{22}	−29.02
Π_3	+2.54

V. CONCLUSIONS

Based on the findings of the experiments and simulations on viscoelastic bodies conducted in recent years, viscoelastic materials are considered to be highly important. However, to date, no KdVB equation has been proposed that describes nonlinear pressure-wave propagation in viscoelastic bodies containing bubbles. In this study, the equation for weakly nonlinear propagation of pressure waves in viscoelastic liquids is derived for the first time while considering the elasticity

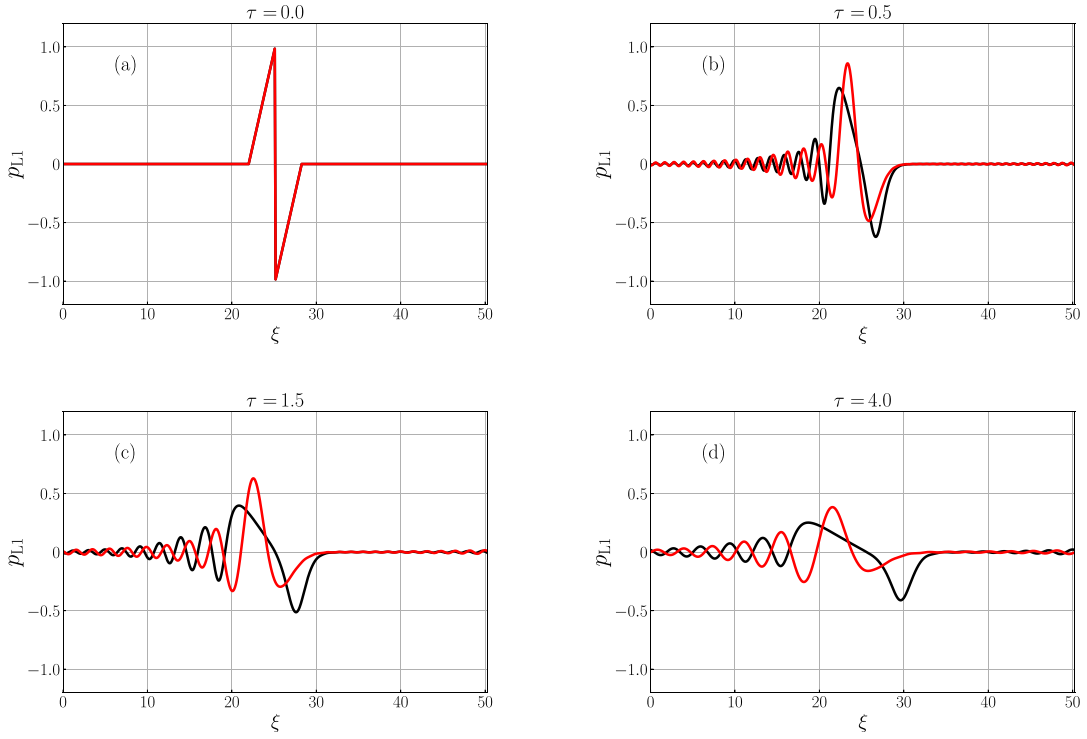

FIG. 3. Temporal evolution of the pressure wave for the case of $\alpha_0 = 1.0 \times 10^{-5}$. The red and black curves represent the waveforms with and without liquid shear elasticity, respectively; ξ is the nondimensional space coordinate, p_{L1} is the first-order perturbation of the liquid pressure, and τ is the nondimensional time: (a) $\tau = 0.0$, (b) $\tau = 0.5$, (c) $\tau = 1.5$, and (d) $\tau = 4.0$. In particular, around the center of Fig. 3(d), a pulse-like waveform was confirmed in the tissue with liquid shear elasticity, whereas a flattened waveform was observed in the tissue without shear elasticity.

of the liquid, and a mathematical model describing the propagation of pressure waves in viscoelastic liquids is presented. By calculating the change of the nonlinear, dissipation, and dispersion effects of pressure waves, we revealed that liquid shear elasticity decreases nonlinear and dissipation effects and increases the dispersion effect. Moreover, we numerically solved the obtained equation to evaluate the changes in pressure wave evolution with and without shear elasticity. Based on the results of the comparison of pressure waveforms between tissues with shear elasticity case and without shear elasticity case, we found that liquid shear elasticity significantly affected the propagation of pressure waves.

Herein, we have presented the nonlinear wave equation that was designed to be applied to biological soft tissues. In the future, we aim to extend the KdVB equation and construct a mathematical model that can be applied to pressure wave propagation in various types of viscoelastic materials. We will also consider the effect of the bulk modulus of the liquid. Moreover, we aim to verify the present KdVB equation and its solutions by comparing the pressure wave obtained from the KdVB equation with that obtained from experiment verification and direct numerical simulation of (1)–(4), (7)–(10), and (12)–(17).

ACKNOWLEDGMENTS

This work was partially carried out with the aid of the JSPS KAKENHI (Grant No. 22K03898), based on results obtained from a project subsidized by the New Energy and Industrial Technology Development Organization (NEDO) (Grant No. JPNP20004), and Ono Charitable Trust for Acoustics, and supported by JKA and its promotion funds from KEIRIN RACE and the Komiya Research Grant from the Turbomachinery Society of Japan. The authors also thank the referees for their valuable comments and suggestions, Editage (www.editage.com) for English language editing, and Takahiro Ayukai for a fruitful discussion.

AUTHOR DECLARATIONS

Conflict of Interest

The authors have no conflicts to disclose.

Author Contributions

T.H. and T.K. contributed equally to this work.

Takeru Hasegawa: Data curation (lead); Formal analysis (equal); Investigation (equal); Methodology (equal); Software (lead); Validation (equal); Visualization (lead); Writing – original draft (equal); Writing – review & editing (equal). **Tetsuya Kanagawa:** Conceptualization (lead); Data curation (supporting); Formal analysis (equal); Funding acquisition (lead); Investigation (equal); Methodology (equal); Project administration (lead); Software (supporting); Supervision (lead); Validation (equal); Visualization (supporting); Writing – original draft (equal); Writing – review & editing (equal).

DATA AVAILABILITY

The data that support the findings of this study are available from the corresponding author upon reasonable request.

APPENDIX A: INHOMOGENEOUS TERMS

The inhomogeneous terms K_i $(i = 1, 2, 3, 4, 5, 6)$ in (49)–(54) are given by

$$K_1 = (3 - s_1)\frac{\partial f}{\partial t_1} - s_2\frac{\partial f}{\partial x_1} + [2s_2(3 - s_1) - 6(s_1 - 2)]f\frac{\partial f}{\partial \varphi_0}, \tag{A1}$$

$$K_2 = -\alpha_0 s_1\frac{\partial f}{\partial t_1} + (1 - \alpha_0)s_3\frac{\partial f}{\partial x_1} - (1 - \alpha_0)V^2 s_4\frac{\partial f}{\partial \varphi_0} - 2\alpha_0 s_1 s_3 f\frac{\partial f}{\partial \varphi_0}, \tag{A2}$$

$$K_3 = -\beta_1(s_2 - s_3)\frac{\partial f}{\partial t_1} + (3 - s_5)p_{G0}\frac{\partial f}{\partial x_1} + \left\{(\beta_1 + \beta_2)s_1(s_2 - s_3) - \beta_1\left(s_2^2 - s_3^2\right) + [3(s_1 - 4) - s_1 s_5 + 6s_5]p_{G0}\right\}f\frac{\partial f}{\partial \varphi_0}, \tag{A3}$$

$$K_4 = \left[\beta_1\alpha_0(s_2 - s_3) - (1 - \alpha_0)s_3\right]\frac{\partial f}{\partial t_1} - (1 - \alpha_0)s_4\frac{\partial f}{\partial x_1} + \left[-2\alpha_0 s_1 s_3 + \beta_1\alpha_0\left(s_2^2 - s_3^2\right) - (\beta_1 + \beta_2)\alpha_0 s_1(s_2 - s_3) + \alpha_0 s_1 s_4 - 2(1 - \alpha_0)s_3^2 + \alpha_0 s_1\left(s_4 + \frac{\Delta^2}{\Omega^2} - [3(\gamma_e - 1) + s_5]p_{G0}\right)\right]f\frac{\partial f}{\partial \varphi_0}, \tag{A4}$$

$$K_5 = \frac{4\mu_{e0}^2}{\Delta^2}f + \left[3(s_5 - 2 + \gamma_e)p_{G0} - 4G - \frac{\Delta^2}{\Omega^2}\right]f^2 + \left(\Delta V\left\{[3(\gamma_e - 1) + s_5]p_{G0} - \frac{\Delta^2}{\Omega^2}\right\} - 4\mu + 4\lambda G\right)\frac{\partial f}{\partial \varphi_0} + \Delta^2\frac{\partial^2 f}{\partial \varphi_0^2}, \tag{A5}$$

$$K_6 = [-3(\kappa - 1) - s_5]\frac{\partial f}{\partial t_1} - \zeta_{STM1}\, s_5 f - \zeta_{STM2}\, s_5\frac{\partial f}{\partial \varphi_0} + [3(\kappa - 1)(3\kappa - 4) + 6(\kappa - 1)s_5 - 3(\kappa - 1)s_2 - s_2 s_5]f\frac{\partial f}{\partial \varphi_0}. \tag{A6}$$

APPENDIX B: NUMERICAL SCHEME

The KdVB equation that is numerically solved is as follows:

$$\frac{\partial f}{\partial \tau} + \frac{\Pi_1}{2}\frac{\partial f^2}{\partial \xi} + \Pi_{21}\frac{\partial^2 f}{\partial \xi^2} + \Pi_3\frac{\partial^3 f}{\partial \xi^3} = 0. \tag{B1}$$

Equation (B1) is separated into two parts: linear equation (B2) and nonlinear equation (B3) as follows:

$$\frac{\partial f}{\partial \tau} + \Pi_{21}\frac{\partial^2 f}{\partial \xi^2} + \Pi_3\frac{\partial^3 f}{\partial \xi^3} = 0, \tag{B2}$$

$$\frac{\partial f}{\partial \tau} + \frac{\Pi_1}{2}\frac{\partial f^2}{\partial \xi} = 0. \tag{B3}$$

First, the linear equation (B2) was analytically solved using the spectral method, and the dependent variables $f_{linear}(\xi, \tau + \Delta\tau)$ were obtained. Next, the nonlinear equation (B3) was calculated using the spectral method and the fourth-order Runge–Kutta method for temporal marching with f_{linear} as the initial condition, and the dependent variables $f(\xi, \tau + \Delta\tau)$ were thereby obtained. The periodic boundary condition was used.

REFERENCES

[1]K. G. Baker, V. J. Robertson, and F. A. Duck, "A review of therapeutic ultrasound: Biophysical effects," Phys. Ther. **81**, 1351 (2001).
[2]G. R. ter Haar, "Therapeutic ultrasound," Eur. J. Ultrasound **9**, 3 (1999).
[3]J. E. Kennedy, G. R. ter Haar, and D. Cranston, "High intensity focused ultrasound: Surgery of the future?," Br. J. Radiol. **76**, 590 (2003).
[4]F. J. Fry, N. T. Sanghvi, R. S. Foster, R. Bihrle, and C. Hennige, "Ultrasound and microbubbles: Their generation, detection and potential utilization in tissue and organ therapy—Experimental," Med. Biol. **21**, 1227 (1995).
[5]S. D. Sokka, R. King, and K. Hynynen, "MRI-guided gas bubble enhanced ultrasound heating in in vivo rabbit thigh," Phys. Med. Biol. **48**, 223 (2003).
[6]Y. Kaneko, T. Maruyama, K. Takegami, T. Watanabe, H. Mitsui, K. Hanajiri, H. Nagawa, and Y. Matsumoto, "Use of a microbubble agent to increase the effects of high intensity focused ultrasound on liver tissue," Eur. Radiol. **15**, 1415 (2005).
[7]F. A. Jolesz, "MRI-guided focused ultrasound surgery," Annu. Rev. Med. **60**, 417 (2009).
[8]L. C. Moyer, K. F. Timbie, P. S. Sheeran, R. J. Price, and G. W. Miller, "High-intensity focused ultrasound ablation enhancement in vivo via phase-shift nanodroplets compared to microbubbles," J. Ther. Ultrasound **3**, 7 (2015).
[9]N. Chang, S. Lu, D. Qin, T. Xu, M. Han, S. Wang, and M. Wan, "Efficient and controllable thermal ablation induced by short-pulsed HIFU sequence assisted with perfluorohexane nanodroplets," Ultrason. Sonochem. **45**, 57 (2018).
[10]E. Vlaisavljevich, K. Lin, M. T. Warnez, R. Singh, L. Mancia, A. J. Putnam, E. Johnsen, C. Cain, and Z. Xu, "Effects of tissue stiffness, ultrasound frequency, and pressure on histotripsy-induced cavitation bubble behavior," Phys. Med. Biol. **60**, 2271 (2015).
[11]E. Vlaisavljevich, J. Greve, X. Cheng, K. Ives, J. Shi, L. Jin, A. Arvidson, T. Hall, T. H. Welling, G. Owens, W. Roberts, and Z. Xu, "Non-invasive ultrasound liver ablation using histotripsy: Chronic study in an *in vivo* rodent model," Ultrasound Med. Biol. **42**, 1890 (2016).
[12]J. E. Lundt, S. P. Allen, J. Shi, T. L. Hall, C. A. Cain, and Z. Xu, "Non-invasive, rapid ablation of tissue volume using histotripsy," Ultrasound Med. Biol. **43**, 2834 (2017).
[13]K. B. Bader, E. Vlaisavljevich, and A. D. Maxwell, "For whom the bubble grows: Physical principles of bubble nucleation and dynamics in histotripsy ultrasound therapy," Ultrasound Med. Biol. **45**, 1056 (2019).
[14]K. J. Pahk, C. Shin, I. Y. Bae, Y. Yang, S. Kim, K. Pahk, H. Kim, and S. J. Oh, "Boiling histotripsy-induced partial mechanical ablation modulates tumour microenvironment by promoting immunogenic cell death of cancers," Sci. Rep. **9**, 9050 (2019).
[15]F. Hasan, K. Mahmud, M. I. Khan, S. Patil, B. H. Dennis, and A. Adnan, "Cavitation induced damage in soft biomaterials," Multiscale Sci. Eng. **3**, 67 (2021).
[16]S. J. Sherwin, L. Formaggia, J. Peiro, and V. Franke, "Computational modeling of 1D blood flow with variable mechanical properties and application to the simulation of wave propagation in the human arterial system," Int. J. Numer. Methods Fluids **43**, 673 (2003).
[17]B. Sturtevant, "Shock wave effects in biomechanics," Sadhana **23**, 579 (1998).
[18]J. V. Kaude, C. M. Williams, M. R. Millner, K. N. Scott, and B. Finlayson, "Renal morphology and function immediately after extracorporeal shock-wave lithotripsy," AJR Am. J. Roentgenol. **145**, 305 (1985).
[19]D. Qin, Q. Zou, S. Lei, W. Wang, and Z. Li, "Nonlinear dynamics and acoustic emissions of interacting cavitation bubbles in viscoelastic tissues," Ultrason. Sonochem. **78**, 105712 (2021).

[20]J. S. Allen and R. A. Roy, "Dynamics of gas bubbles in viscoelastic fluids—I: Linear viscoelasticity," J. Acoust. Soc. Am. **107**, 3167 (2000).
[21]X. Yang and C. C. Church, "A model for the dynamics of gas bubbles in soft tissue," J. Acoust. Soc. Am. **118**, 3595 (2005).
[22]R. Gaudron, M. T. Warnez, and E. Johnsen, "Bubble dynamics in a viscoelastic medium with nonlinear elasticity," J. Fluid Mech. **766**, 54 (2015).
[23]F. Hamaguchi and K. Ando, "Linear oscillation of gas bubbles in a viscoelastic material under ultrasound irradiation," Phys. Fluids **27**, 113103 (2015).
[24]C. Hua and E. Johnsen, "Nonlinear oscillations following the Rayleigh collapse of a gas bubble in a linear viscoelastic (tissue-like) medium," Phys. Fluids **25**, 083101 (2013).
[25]E. Vlaisavljevich, A. Maxwell, M. Warnez, E. Johnsen, C. A. Cain, and Z. Xu, "Histotripsy-induced cavitation cloud initiation thresholds in tissues of different mechanical properties," IEEE Trans. Ultrason. Ferroelectr. Freq. Control **61**, 341 (2014).
[26]C. T. Wilson, T. L. Hall, E. Johnsen, L. Mancia, M. Rodriguez, J. E. Lundt, T. Colonius, D. L. Henann, C. Franck, Z. Xu, and J. Sukovich, "Comparative study of the dynamics of laser and acoustically generated bubbles in viscoelastic media," Phys. Rev. E **99**, 043103 (2019).
[27]J. Zimberlin, N. Sanabria-Delong, and G. N. Tew, "Cavitation rheology for soft materials," Soft Matter **3**, 763 (2007).
[28]L. Pavlovsky, M. Ganesan, and J. G. Younger, "Elasticity of microscale volumes of viscoelastic soft matter by cavitation rheometry," Appl. Phys. Lett. **105**, 114105 (2014).
[29]S. Hutchens, S. Fakhouri, and A. Crosby, "Elastic cavitation and fracture via injection," Soft Matter **12**, 2557 (2016).
[30]A. Delbos, J. L. Cui, S. Fakhouri, and A. Crosby, "Cavity growth in a triblock copolymer polymer gel," Soft Matter **8**, 8204 (2012).
[31]L. E. Jansen, N. P. Birch, and J. D. Schiffman, "Mechanics of intact bone marrow," J. Mech. Behav. Biomed. Mater. **50**, 299 (2015).
[32]S. Kundu and A. Crosby, "Cavitation and fracture behavior of polyacrylamide hydrogels," Soft Matter **5**, 3963 (2009).
[33]C. S. Peel, X. Fang, and S. R. Ahmad, "Dynamics of laser-induced cavitation in liquid," Appl. Phys. A **103**, 1131 (2011).
[34]A. Jamburidze, M. D. Corato, A. Huerre, A. Pommella, and V. Garbin, "High-frequency linear rheology of hydrogels probed by ultrasound-driven microbubble dynamics," Soft Matter **13**, 3946 (2017).
[35]L. van Wijngaarden, "One-dimensional flow of liquids containing small gas bubbles," Annu. Rev. Fluid Mech. **4**, 369 (1972).
[36]T. Yatabe, T. Kanagawa, and T. Ayukai, "Theoretical elucidation of effect of drag force and translation of bubble on weakly nonlinear pressure waves in bubbly flows," Phys. Fluids **33**, 033315 (2021).
[37]T. Kanagawa, T. Ayukai, T. Maeda, and T. Yatabe, "Effect of drag force and translation of bubbles on nonlinear pressure waves with a short wavelength in bubbly flows," Phys. Fluids **33**, 053314 (2021).
[38]S. Arai, T. Kanagawa, and T. Ayukai, "Nonlinear pressure waves in bubbly flows with drag force: Theoretical and numerical comparison of acoustic and thermal and drag force dissipations," J. Phys. Soc. Jpn. **91**, 043401 (2022).
[39]E. Zilonova, M. Solovchuk, and T. W. H. Sheu, "Dynamics of bubble-bubble interactions viscoelastic drag," Phys. Rev. E **99**, 023109 (2019).
[40]R. Egashira, T. Yano, and S. Fujikawa, "Linear wave propagation of fast and slow modes in mixtures of liquid and gas bubbles," Fluid Dyn. Res. **34**, 317 (2004).
[41]T. Yano, R. Egashira, and S. Fujikawa, "Linear analysis of dispersive waves in bubbly flows based on averaged equations," J. Phys. Soc. Jpn. **75**, 104401 (2006).
[42]T. Yano, T. Kanagawa, M. Watanabe, and S. Fujikawa, "Nonlinear wave propagation in bubbly liquids," in *Shock Wave Science and Technology Reference Library* (Springer, 2013).
[43]A. V. Jones and A. Prosperetti, "On the suitability of first-order differential models for two-phase flow prediction," Int. J. Multiphase Flow **11**, 133 (1985).
[44]I. Eames and J. C. R. Hunt, "Forces on bodies moving unsteadily in rapidly compressed flows," J. Fluid Mech. **505**, 349 (2004).
[45]Z. D. Zhang and A. Prosperetti, "Ensemble-averaged equations for bubbly flows," Phys. Fluids **6**, 2956 (1994).
[46]J. B. Estrada, C. Barajas, D. L. Henann, and E. Johnsen, "High strain-rate soft material characterization via inertial cavitation," J. Mech. Phys. Solids **112**, 291 (2018).
[47]J. B. Keller and I. I. Kolodner, "Damping of underwater explosion bubble oscillations," J. Appl. Phys. **27**, 1152 (1956).
[48]J. B. Keller and M. Michael, "Bubble oscillations of large amplitude," J. Acoust. Soc. Am. **68**, 628 (1980).
[49]T. Kamei, T. Kanagawa, and T. Ayukai, "An exhaustive theoretical analysis of thermal effect inside bubbles for weakly nonlinear pressure waves in bubbly liquids," Phys. Fluids **33**, 053302 (2021).
[50]T. Kanagawa and T. Kamei, "Thermal effect inside bubbles for weakly nonlinear pressure waves in bubbly liquids: Theory on short waves," Phys. Fluids **33**, 063319 (2021).
[51]S. Kagami and T. Kanagawa, "Weakly nonlinear propagation of focused ultrasound in bubbly liquids with a thermal effect: Derivation of two cases of Khokolov–Zabolotskaya–Kuznetsoz equations," Ultrason. Sonochem. **88**, 105911 (2022).
[52]A. Prosperetti, "The thermal behaviour of oscillating gas bubbles," J. Fluid Mech. **222**, 587 (1991).
[53]K. Sugiyama, S. Takagi, and Y. Matsumoto, "A new reduced-order model for the thermal damping effect on radial motion of a bubble (1st report, perturbation analysis)," Trans. JSME, Ser. B **71**, 1011 (2005).
[54]P. N. T. Wells and H. Liang, "Medical ultrasound: Imaging of soft tissue strain and elasticity," J. R. Soc. Interface **8**, 1521 (2011).
[55]E. Zilonova, M. Solovchuk, and T. W. H. Sheu, "Bubble dynamics in viscoelastic soft tissue in high-intensity focal ultrasound thermal therapy," Ultrason. Sonochem. **40**, 900 (2018).
[56]M. Ichihara, H. Ohkunitani, Y. Ida, and M. Kameda, "Dynamics of bubble oscillation and wave propagation in viscoelasti liquids," J. Volcanol. Geotherm. Res. **129**, 37 (2004).
[57]Y. Zheng, X. Chen, A. Yao, H. Lin, Y. Shen, Y. Zhu, M. Lu, T. Wang, and S. Chen, *Shear Wave Propagation in Soft Tissue and Ultrasound Vibrometry* (InTech, 2013).
[58]V. Suomi, Y. Han, E. Konofagou, and R. Cleveland, "The effect of temperature dependent tissue parameters on acoustic radiation force induced displacements," Phys. Med. Biol. **61**, 7427 (2016).
[59]M. Orosz, G. Molnarka, and E. Monos, "Curve fitting methods and mechanical models for identification of viscoelastic parameters of vascular wall—A comparative study," Med. Sci. Monit. **3**, 599 (1997).
[60]T. Sumi and T. Hashimoto, "An estimation of dynamic properties of viscoelastic materials via inverse analysis on inertial micro cavitation," J. Soc. Rheol. Jpn. **50**, 137 (2022).
[61]T. Kanagawa, T. Yano, M. Watanabe, and S. Fujikawa, "Unified theory based on parameter scaling for derivation of nonlinear wave equations in bubbly liquids," J. Fluid Sci. Technol. **5**, 351 (2010).
[62]H. Joodaki and M. B. Panzer, "Skin mechanical properties and modeling: A review," Proc. Inst. Mech. Eng., Part H **232**, 323 (2018).
[63]A. L. McKnight, J. L. Kugel, and P. J. Rossman, "MR elastography of breast cancer: Preliminary results," AJR Am. J. Roentgenol. **178**, 1411 (2002).
[64]A. Jeffrey and T. Kawahara, *Asymptotic Methods in Nonlinear Wave Theory* (Pitman, London, 1982).
[65]G. M. Muslu and H. A. Erbay, "A split-step Fourier method for the complex modified Korteweg-de Vries equation," Comput. Math. Appl. **45**, 503 (2003).
[66]T. Ayukai and T. Kanagawa, "Numerical study on nonlinear evolution of pressure waves in bubbly liquids: Effective range of initial void fraction," Proc. Meet. Acoust. **39**, 045009 (2019).
[67]D. Fuster, J. M. Conoir, and T. Colonius, "Effect of direct bubble-bubble interactions on linear-wave propagation in bubbly liquids," Phys. Rev. E **90**, 063010 (2014).
[68]D. Fuster and F. Montel, "Mass transfer effects on linear wave propagation in diluted bubbly liquids," J. Fluid Mech. **779**, 598 (2015).